Using Multiple-Mode Models for Fitting and Predicting Rheological Properties of Polymeric Melts

B. Jiang, P. A. Kamerkar, D. J. Keffer, B. J. Edwards

Department of Chemical Engineering, University of Tennessee, Knoxville, Tennessee 37996-2200

Received 23 August 2003; accepted 21 March 2005
DOI 10.1002/app.22486
Published online in Wiley InterScience (www.interscience.wiley.com).

ABSTRACT: Several classes of multiple-mode rheological constitutive equations are tested for fitting and predicting viscoelastic flow properties of a typical low-density polyethylene melt. An optimization procedure is used to fit the phenomenological parameters of each model under consideration to experimental data taken in small-amplitude oscillatory shear flow and steady shear flow. These parameter values are then used to generate predictions for transient shear and uniaxial elongational flow experiments, and the predictions are then compared to experimental data. Model successes and failures are discussed, and the outlook for using rheological equations in real design processes is addressed. © 2005 Wiley Periodicals, Inc. J Appl Polym Sci 99: 405–423, 2006

Key words: nonlinear polymers; polymer melts; rheology; viscoelastic properties

INTRODUCTION

For many years, one overall goal of theoretical rheologists has been to obtain a level of understanding of material behavior sufficient to allow for the prediction of viscoelastic properties in arbitrary flow fields. After approximately 75 years of effort spent in pursuit of this goal, it is still largely unachieved, even for isothermal cases. In recent years, modeling efforts have intensified as theoretical developments, such as reptation theory, mature, and as computational power has increased. It is now time to assess, in general terms, how close rheologists are to achieving this goal.

In this article, we offer a current assessment of the potential predictive capabilities of viscoelastic fluid models. Rather than focusing on the particular models popular today (which might not be popular a decade from now), we examine instead semiphenomenological models (i.e., models involving empirical parameters) that characterize a certain class of model types. This allows us to judge the capabilities of the class using the simplest possible methodology, that is, without getting caught up in model-specific peculiarities and complexities. Suffice it to mention that all of today's popular models fall into one of the model classes examined herein, with one caveat: since we are examining polymer melts, which have a spectrum of relaxation times, we are only examining multiple-mode versions of viscoelastic fluid models. We see no point in trying to fit and predict nonlinear viscoelastic properties if the linear ones cannot be fit accurately. Since single-mode models are incapable of matching linear viscoelastic data from polymer melts in a quantitative fashion, it is apparent that we need only consider herein multi-mode versions of the chosen model classes.

The strategy of the research reported in this article is to fit the models examined herein to a limited amount of easily obtained experimental data of a typical polymer melt, and then to test how well each quantitatively predicts experimental data to which the inherent model parameters were not explicitly fit. The methodology used to fit the model parameters to the requisite amount of experimental data is now easily implemented using standard desktop computers. This methodology was described in detail in a prior publication,[1] so only a brief summary will be included below. In the prior publication, only a single model class was examined, as the point of that article was to develop the methodology. Here, we wish to apply this methodology to draw more general conclusions.

The model classes examined in the succeeding sections are the following. The most basic semiphenomenological model class is that of the uncoupled (i.e., no coupling between the various relaxation modes), linear relaxation models with constant relaxation times. The most well known and widely used of these is the multi-mode Upper-Convected Maxell Model, and thus we examine it herein. Of course, this model has

Correspondence to: B. J. Edwards (bjedwards@chem.engr.utk.edu).

Contract grant sponsor: Chemical Engineering Department at the University of Tennessee.

no hope of fitting any nonlinear viscoelastic properties; however, we examine it as a basis for the linear viscoelastic response exhibited by many other models in the linear limit. The second class is that of uncoupled, linear relaxation models with variable relaxation times. Examples of models falling into this group are the Phan-Thien/Tanner Model,[2] the Modified Upper-Convected Maxwell Model,[3] and the Extended White/Metzner Model[4] (EWMM). Herein, we examine a version of the EWMM (as defined below) as an apt representation of this class. The third class is that of uncoupled, nonlinear relaxation models. The example of this class studied herein is the most well-known model of this type, the Giesekus Model.[5]

The remaining two classes of viscoelastic fluid models examined herein are those that involve coupled relaxation modes, that is, the modes are no longer taken to be independent of each other, as was the case in all examples considered above. The first remaining class is that of the pair-wise coupled relaxation modes models, that is, when each mode is taken to couple to one, and only one, other relaxation mode. The second remaining class is that in which each mode of a given model is allowed to interact with every other mode. Although it seems obvious that the first class is merely a special case of the second, we make the distinction between these two classes for the following reason: many recently developed viscoelastic fluid models were written in terms of two relaxation modes, and these modes are coupled with each other. To fit experimental data, more than 2 modes are needed; hence, these models are generally duplicated the requisite number of times, thus producing a pair-wise coupled model. (As an example, the fitting capabilities of the Pom-Pom Model[6–8] were investigated recently using 12 modes.[9,10] The multiple-mode version of this model falls into the class of pair-wise coupled modes with nonlinear extensions—see below.) Obviously, this is just a special case of the more general fully-coupled models, but it is interesting to examine pair-wise coupling as an entity unto itself because this class possesses some striking peculiarities[1]—see below for more details. The models examined herein for both of these classes are the semiphenomenological multiple-mode models introduced by Beris and Edwards[11]; these were chosen as the simplest possible representations of this class of models.

Literature overview

Of course, this is not the first study aimed at fitting and predicting rheological properties of polymeric fluids. One of the first and most extensive tests of rheological constitutive equations was that of Quinzani et al.,[12] who examined the fitting capabilities of several multiple-mode rheological models (using 4 modes), including the Giesekus Model, for a vast array of experimental measurements of polyisobutylene solutions. Results of this study were encouraging for the future, but were limited by the simplicity of the models examined therein.

With regard to polymer melts, an international consortium has recently undertaken the task of matching experimental polymer processing flows to numerical simulations.[13] Efforts with multiple-mode Giesekus and Phan-Thien/Tanner Models (with 4–9 modes) have yielded reasonable predictions of process flow characteristics.[14,15] As already mentioned, several investigations of the predictive capabilities of the Pom-Pom Model (with 8–12 modes) have also already been published, with impressive results.[8–10]

EXPERIMENTAL

All experimental data used in this investigation were taken using standard rheological testing equipment and procedures at the University of Tennessee. Results presented below are for a typical, industrially relevant, low-density polyethylene (LDPE) sample at 175°C. The LDPE sample was obtained from Exxon, having been prepared using a Ziegler–Nata catalyst. It has a wide molecular weight distribution, with a value of the polydispersity index of 5.15. The value of the melt index was 0.2 g/min, with a density of 0.923 g/cm^3. The weight-average molecular weight, according to gel permeation chromatography, was 80,350 g/mol.

A variety of experimental data were obtained, as described in a preceding article.[1] A dynamic frequency sweep was performed in the range of 0.01s^{-1}–100 s^{-1}. From this, the storage modulus (G') and loss modulus (G'') data in small-amplitude oscillatory shear flow (SAOSF) were obtained. Shear viscosity data were taken over seven decades of shear rates (0.01 s^{-1}–100,000 s^{-1}). Steady-state first normal stress difference data covering a fraction of this shear-rate range were also obtained, along with transient shear stress data (start up and relaxation) and first normal stress difference data. Transient elongational viscosity measurements were made using four semihyperbolically converging dies of Hencky strains 4, 5, 6, and 7, in the manner described in Ref. 16. We would expect this elongational viscosity data to be accurate for this particular polymer melt at this temperature and strain rate regime.[17]

Optimization methodology

To place all models on an even footing, we took the number of modes used in each model as 6. This number was chosen because it allowed a fit of the storage and loss moduli of the polymer melt used in this study to about 5% relative root-mean-square (RMS) error

TABLE I
Number of Fitting Parameters for Each Model Investigated in this Study. (See text for acronym definitions.)

Model	UMM	UMM-EWM	UGM	PCMM	PCMM-EWM	FCMM	FCMM-EWM
Number of parameters	12	18	18	15	21	42	48

using the *PADLAP* program of Simhambhatla and Leonov[18]; thus, we hypothesize (as rationalized below) that 6 modes should be sufficient for fitting most nonlinear properties for this particular polymer melt as well. (See below for more details concerning the *PADLAP* fit to the experimental data.)

The overall optimization strategy of this investigation is to fit exactly 6 modes of a given model to the dynamic moduli (in SAOSF) and steady-state viscosity and first normal stress coefficient (in steady shear flow), and then to check whether the model predicts well the remaining experimental data. Each model examined below contains a definite number of parameters, which must be fit to the specified data set. The number of parameters fitted for each model investigated herein is listed in Table I. (See below for acronym definitions.)

For each model investigated, a set of coupled, ordinary differential equations (ODEs) quantify the time evolution of the independent, nonvanishing elements of the mode stress tensors in homogeneous flow fields. For fixed values of the model parameters, a fourth-order Runge–Kutta method is used to solve the set of coupled ODEs. At steady state, the Newton–Raphson Method is applied to solve the resulting nonlinear algebraic equations. For all models examined herein, the dynamic moduli in SAOSF can be calculated analytically.

The technique used to optimize the model parameters was the Nelder and Mead Downhill Simplex Method (NMDSM), which requires only functional evaluations, not derivatives.[19] Although this optimization technique is not very efficient in terms of the number of functional evaluations and computational effort required, the NMDSM will always find a minimum, provided that one exists. However, the NMDSM is not guaranteed to find the global minimum, which creates a challenge for its users. Insight into the physical significance of the parameters and an understanding of the underlying physics is thus crucial to obtaining a good initial guess to the optimization problem. Multiple initial guesses are required to test whether the resulting minimum is indeed the global minimum. As the dimensions of the parameter space increase when the number of mode pairs increases, optimization using this method can require substantial computational time. As reported in Ref. 1, this method appears to give adequate results for this type of parameter fitting. Thus, we continue to use it in this investigation. It has the further benefit of being very simple to implement, thus making this methodology available to any engineer with basic programming skills.

The constraints on the parameters have already been discussed.[1] For the parameters common to all models, that is, the relaxation times, $\lambda_i(s)$, and the concentrations, n_i (mol/m^3), of each mode, the constraints are that each quantity is a positive entity. Constraints on parameters that are peculiar to the various models investigated herein are discussed later.

We used the following expression for the objective function, F_{obj}, which was the function minimized by the NMDSM:

$$F_{obj} = \sqrt{\frac{\sum_{j=1}^{n_{type}} \sum_{i=1}^{n_j} w_{i,j} \left(\frac{R_{i,j,\mathrm{exp}} - R_{i,j,\mathrm{model}}}{R_{i,j,\mathrm{exp}}} \right)^2}{\sum_{j=1}^{n_{type}} \sum_{i=1}^{n_j} w_{i,j}}}. \qquad (1)$$

In this expression, n_{type} is the number of data types (types of data for the present article are the dynamic moduli, as well as the steady-state shear viscosity and first normal stress coefficient), n_j is the number of data points of a specific type of data, $w_{i,j}$ is the weight factor of the corresponding data, and **R** is the value of either the experiment or model.

Since the dimension of solution space can be quite large, the method used to obtain a reasonable initial guess is vital to the optimization code. Generally, we fit the dynamic moduli data from the SAOSF experiment by varying λ_i and n_i for $i = 1,\ldots,6$. We used initial guesses for the relaxation times with incremental orders of magnitude. Furthermore, for initial guesses of the modal concentrations, we chose values that were very close to zero. Once the dynamic moduli data were fit well, we then used the converged values of the parameters as an initial guess to fit simultaneously both steady-state shear viscosity and dynamic moduli data. Finally, we also used the optimized parameter set from the previous step as the initial guess to fit simultaneously three sets of experimental data, including: dynamic moduli, steady-state shear viscosity, and steady-state first normal stress coefficient. We did not include

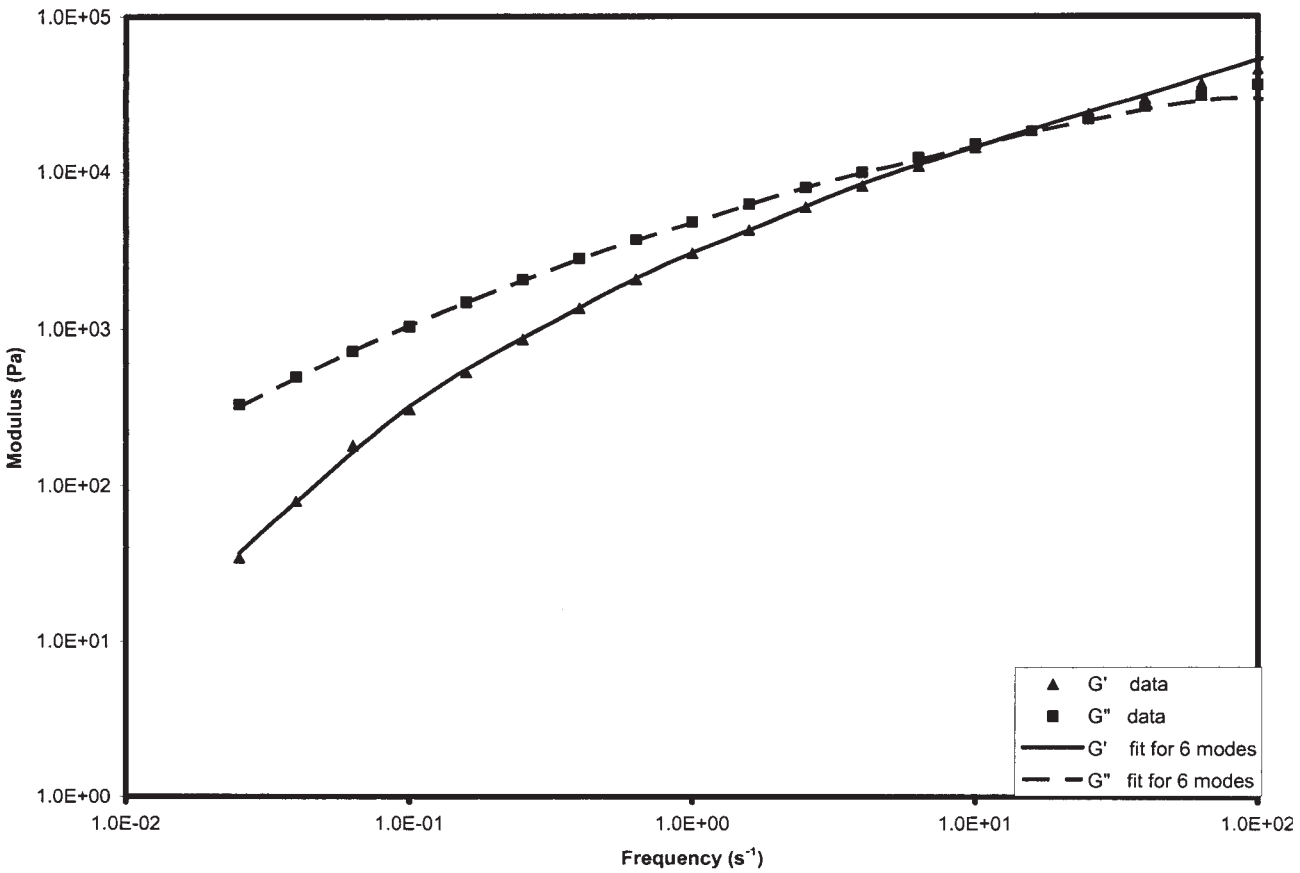

Figure 1 Fit of the Padé-Laplace program *PADLAP* to experimental data of the dynamic moduli in SAOSF. See Table II for parameter values.

the experimental data for the transient shear stress or first normal stress difference among the data that we fit, nor the transient uniaxial elongational viscosity data.

Over the past few decades, several different methods have been put forth for fitting rheological models (typically composed of uncoupled Maxwell modes) to linear viscoelastic data.[18,20–24] Over time, these methods have generally become more sophisticated as computational capabilities have increased, and have done a better job of fitting parameters with smaller RMS error. These methods are, however, not easily generalized to cases involving nonlinear viscoelastic data and more complicated rheological models. Such methods that do exist for fitting nonlinear viscoelastic data suffer from a lack of sophistication. We are not addressing the issue of sophistication in this article; we want to employ a crude optimization methodology to examine what is possible for the average industrial polymer engineer to achieve with a given rheological model.

To examine whether or not our optimization technique is sufficient for this application, we must compare it with one of the sophisticated methods mentioned above. Those methods, as discussed above, are only for linear viscoelastic data. Although there is no basis of comparison for nonlinear viscoelastic data, we can compare our methodology to prior optimization methods for the linear data. In Figure 1, we present the dynamic moduli data of the LDPE sample described above in the SAOSF experiment, along with a fit of 6 uncoupled Maxwell modes using the Padé-Laplace methodology of Simhambhatla and Leonov,[18] according to the authors' *PADLAP* program. The RMS error of this sophisticated fit is less than 5%, which is quite good. We believe that 6 modes is the minimum number needed by this method to get a very good fit of the experimental data. The parameter values obtained from the optimization routine are presented in Table II. Suffice it to say that the exact same fit can be obtained using the optimization routine developed in this work. Furthermore, for the 6-mode version of the Upper-Convected Maxwell Model used herein, not only is the fit the same as in the more sophisticated code, but the parameter values obtained are essentially the same as well (within 1% RMS error). Thus, we conclude that, at least as far as the linear viscoelasticity data are concerned, our optimization methodology is sufficient to the task under consideration.

TABLE II
Parameter Values Determined by the Padé-Laplace Method Using the *PADLAP* Program

Mode no.	1	2	3	4	5	6
λ_i (s)	1.000E−2	5.248E−2	2.754E−1	1.445	7.586	3.981E+1
n_i (mol/m^3)	1.441E+1	4.260	2.208	6.880E−1	1.781E−1	4.959E−3

Uncoupled linear relaxation models with constant relaxation times

The example tested under this class of viscoelastic fluid models is the Uncoupled Maxwell Modes (UMM) Model, which is composed of 6 Upper-Convected Maxwell Modes. Beforehand, we were aware of the well-known deficiencies of this model for fitting nonlinear viscoelasticity data, but we examine its behavior here as a base case, since all other models tested herein reduce to it in the linear, uncoupled modes limit.

The UMM Model equations are expressed in terms of six uncoupled evolution equations for the 6 mode stress tensors, σ^i, $i = 1,\ldots,6$:

$$\sigma^i_{\alpha\beta} + \lambda_i \hat{\sigma}^i_{\alpha\beta} = 2 n_i N_A k_B T \lambda_i A_{\alpha\beta}, \tag{2}$$

where the upper-convected derivative is defined as

$$\hat{\sigma}^i_{\alpha\beta} \equiv \frac{\partial \sigma^i_{\alpha\beta}}{\partial t} + v_\gamma \nabla_\gamma \sigma^i_{\alpha\beta} - \sigma^i_{\alpha\gamma} \nabla_\gamma v_\beta - \sigma^i_{\beta\gamma} \nabla_\gamma v_\alpha. \tag{3}$$

In the above expressions, k_B is Boltzmann's constant, T is the absolute temperature, N_A is Avogadro's number, and $A_{\alpha\beta} = (\nabla_\alpha v_\beta + \nabla_\beta v_\alpha)/2$ is the symmetric part of the velocity gradient tensor field. The total extra stress in the fluid is then expressed as the sum overall of the mode stress tensors:

$$\sigma_{\alpha\beta} = \sum_{i=1}^{6} \sigma^i_{\alpha\beta}. \tag{4}$$

This equation set can be used to calculate the rheological properties of the polymer following standard definitions. The storage and loss moduli in SAOSF can be expressed as

$$G'(\omega) = \sum_{i=1}^{6} \frac{\eta_i \lambda_i \omega^2}{1 + (\lambda_i \omega)^2}, \tag{5}$$

$$G''(\omega) = \sum_{i=1}^{6} \frac{\eta_i \omega}{1 + (\lambda_i \omega)^2}, \tag{6}$$

respectively, where ω is the angular frequency of the SAOSF and $\eta_i = n_i N_A k_B T \lambda_i$.

In steady shear flow, the shear viscosity (η) of the UMM Model is independent of the shear rate, as is the first normal stress coefficient (Ψ_1). Consequently, we have no hope of fitting the shear-thinning behavior exhibited by this LDPE, and therefore we perform the optimization by fitting the model parameters to the SAOSF data and the Newtonian plateau for η at low shear rates. The parameter values thus obtained are reported in Table III. They are significantly different from those found using the *PADLAP* program, which is due to the fact that we have used the steady-shear data in the optimization as well as the SAOSF data. This is also an indication that the *PADLAP* parameters cannot be used to model accurately steady shear flow. It raises the question as to whether or not the relaxation times determined using only SAOSF have any meaning outside of SAOSF; it is well-known that the parameterization of linear viscoelastic flow data is an ill-posed mathematical problem.[20]

The fit of the UMM Model to the experimental data for the dynamic moduli (G' and G'') versus frequency in the SAOSF experiment is virtually indistinguishable from that displayed in Figure 1. The fit is very good, and the RMS error is less than 5%.

In Figure 2, we plot the experimental data and the fit with the UMM Model for the steady-state shear viscosity versus shear rate. With this model, we can only fit the Newtonian plateau at low shear rates; however,

TABLE III
List of Parameters for All Modes of the UMM Model Used To Fit the Data of SAOSF and Shear Viscosity at Low Shear Rates

Mode no.	1	2	3	4	5	6
λ_i (s)	1.108E−3	4.237E−3	4.082E−2	2.487E−1	1.435	9.583
n_i (mol/m^3)	7.456E−9	2.455E+1	5.995	2.337	7.862E−1	1.448E−1

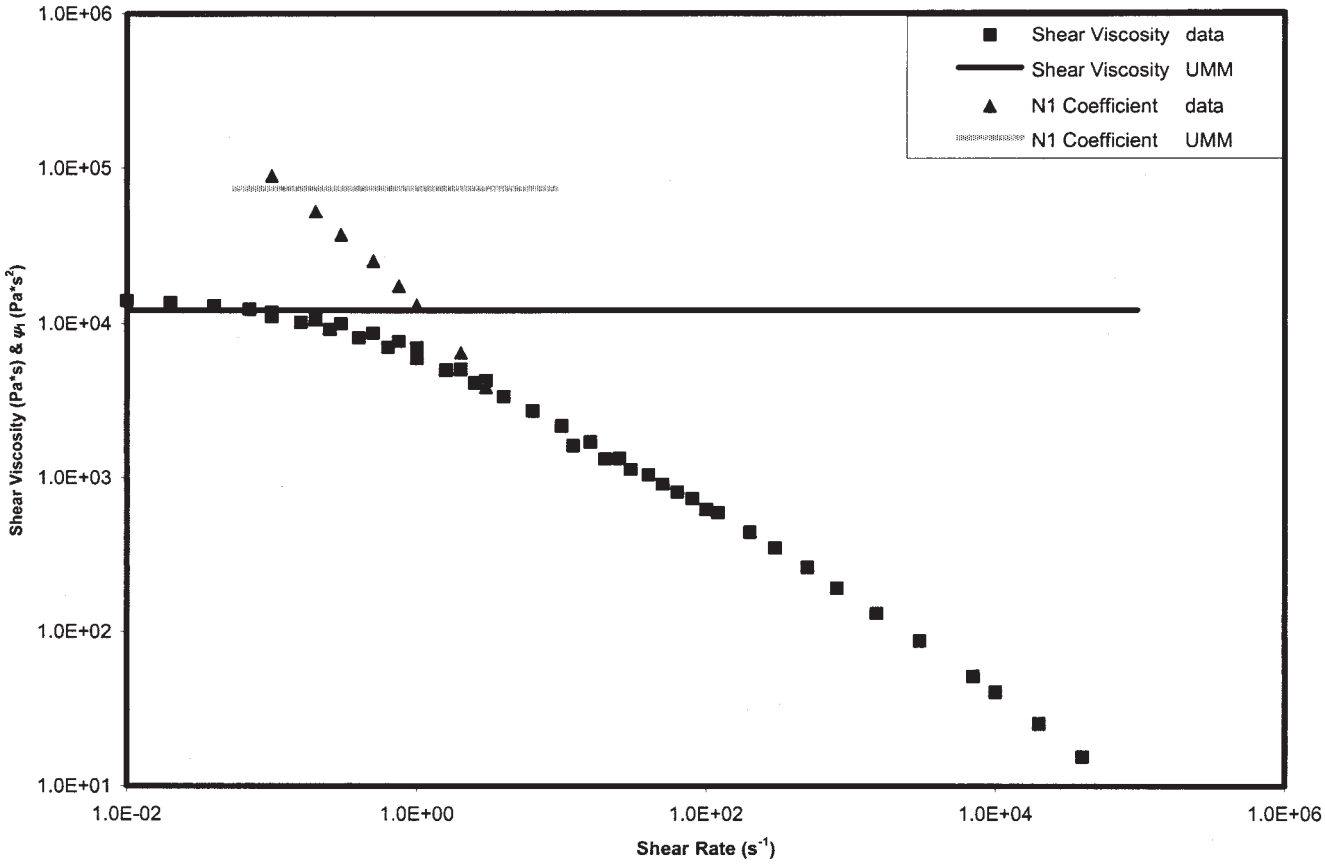

Figure 2 Steady-state shear viscosity and first normal stress coefficient versus shear rate, as fitted with the UMM Model.

the Figure indicates that it is possible to do this simultaneously with fitting the SAOSF data. Also in Figure 2, the model prediction is given for the first normal stress coefficient as a function of shear rate. As is well known, the UMM Model predicts a constant value of Ψ_1. Therefore, we have no hope of predicting anything other than the Newtonian plateau value of this quantity at low shear rates; perhaps surprisingly, the value predicted is not too far off from the experimental value. Of course, the value of Ψ_2 predicted by this model is zero for all shear rates.

Since the UMM Model cannot fit the shear-thinning behavior of either η or Ψ_1, there is no point in trying to predict the transient steady-shear data in this regime. Our conclusion is thus that the UMM Model cannot be used to predict nonlinear rheological behavior in shear flow, although it is possible to get good results within the linear regime.

In Figure 3, we plot UMM Model predictions for the uniaxial elongational viscosity versus time for different elongational strain rates. For comparison purposes, the experimental Trouton curve (3η at $\dot{\gamma} = 0.01$ s^{-1}) and its UMM Model prediction in steady shear flow are plotted as well. This figure demonstrates that the UMM Model generally reflects the trend of change of elongational viscosity versus time and strain rate in the region studied, although the errors between theoretical results and experimental data are huge. Furthermore, the steady-state values of the viscosity predicted by the UMM Model are obviously going to be way too high.

Uncoupled linear relaxation models with variable relaxation times

The Uncoupled Extended White/Metzner (UEWM) Model is a variation of the UMM Model wherein the mode relaxation times are no longer treated as constants. In this model, each mode relaxation time is taken as a function of the corresponding mode stress tensor. Here, we choose the following relationship to express this functional dependency:

$$\lambda_i = \lambda_{0,i}\left(\mathrm{tr}\left(\frac{\sigma^i}{n_i K_B T}\right) + 1\right)^{k_i}, \tag{7}$$

where $k_i \leq 0$, which is similar in spirit and practice to the relationship of Souvaliotis and Beris.[4] We chose this slightly different functional form of eq. (7) because it seems to give a somewhat smoother description of steady shear flow properties than the one originally

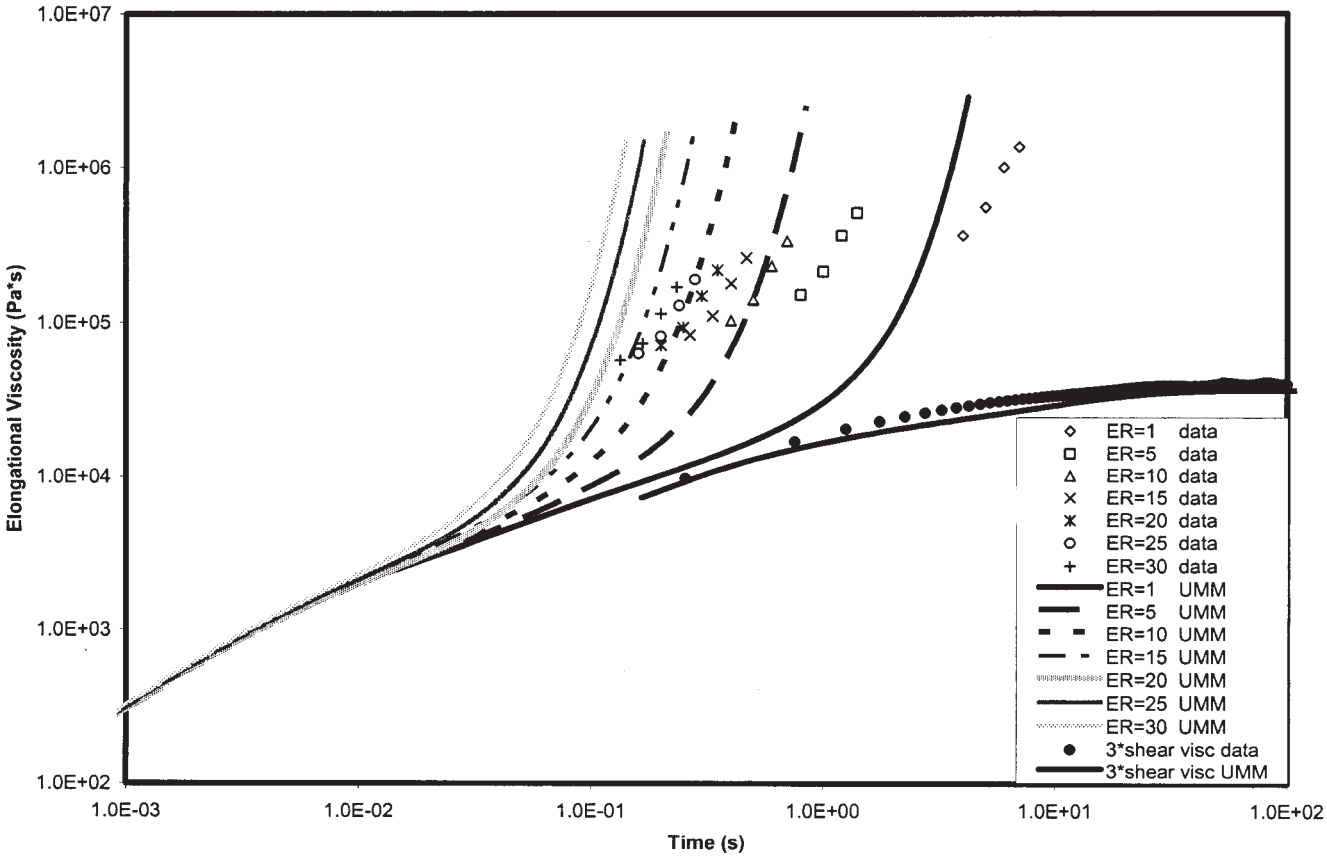

Figure 3 Elongational viscosity as a function of time, as predicted with the UMM Model. ER refers to the strain rate, in units of reciprocal seconds.

proposed by the former authors. Note that other than this small change, all other equations from the preceding section carry over to this case. Consequently, the UEWM Model will reduce to the UMM Model when all of the k_i are equal to zero.

As described in the section on optimization, we fit the parameters of the UEWM Model to experimental data of SAOSF, steady-shear viscosity, and first normal stress coefficient. Then, we predict the rheological properties of polymer melts in transient shear and uniaxial elongational flows using the corresponding parameters acquired through the data fitting. The parameter values obtained through the fitting are reported in Table IV.

As for the SAOSF experimental data, the fit achieved here is not quite as good as in the previous two cases, but it is still less than 10% RMS error. (See Table V for a compilation of RMS errors for this study.) Figure 4 displays the fits to the steady shear viscosity and first normal stress coefficient. The fits are quite decent, with associated RMS errors of roughly 8 and 6%, respectively. Note that the steady shear viscosity is fitted over seven decades of shear rate. Obviously, this model does a much better job of fitting steady shear data than the UMM Model, which is strictly linear. The prediction for the second normal stress coefficient is again zero, since the UEWM Model does nothing to correct this inadequacy of the UMM Model. (See Table VI for zero shear-rate values of Ψ_2/Ψ_1.)

We plot the shear stress (SS) and first normal stress difference (N_1) versus time for transient shear flow at

TABLE IV
List of Parameters for All Modes of the UEWM Model Used To Fit the Experimental Data of Dynamic Moduli, Shear Viscosity, and First Normal Stress Coefficient

Mode no.	1	2	3	4	5	6
$\lambda_{0,i}$ (s)	1.000E−8	9.288E−3	1.854E−2	1.191E−1	1.054	8.978
n_i (mol/m^3)	6.925E−10	1.811E+1	8.782E−19	4.649	1.067	2.206E−1
k_i	−7.573E−7	−2.004	−6.184E−16	−1.994E+1	−1.492	−4.796E−1

TABLE V
The Relative Root-Mean-Square (RMS) Error (%) of Different Curves Attained by Different Models. Note that the first three columns are fits, and the last three columns are predictions.

Model	Complex modulus	Steady-state shear viscosity	Ψ_1	Elongational viscosity	Transient shear stress ($\dot{\gamma}$ = 0.5 & 1.0 s^{-1})	Transient N_1 ($\dot{\gamma}$ = 0.5 & 1.0 s^{-1})
UMM	2.20	16,000	1,200	63,300	271	482
UEWM	9.38	8.04	6.25	94.8	18.5	51.2
UGM	4.78	8.59	7.68	49.3	7.60	130
PCMM	24.4	26.1	26.5	6,670	41.2	128
PCMM-EWM	11.5	6.28	7.11	51,400	24.1	54.1
FCMM	23.4	26.2	26.7	7,230	31.5	124
FCMM-EWM	2.71	5.47	12.7	841	11.8	126

$0.5s^{-1}$ and $1.0s^{-1}$, respectively, in Figures 5 and 6. These plots are presented logarithmically, which accentuates the differences between the theoretical predictions and the experimental data at very short and very long times. Data were taken at shear rates ranging from 0.01 to $5s^{-1}$, with similar results obtained as those reported herein. In both cases, the shear stress transients at flow start-up and cessation are predicted fairly well, with only a slight under-prediction of the overshoot upon start-up. The prediction of the first normal stress difference fares well over most of the time range examined, but fails quantitatively at both short and long times. The model over-predicts N_1 at low times, and under-predicts it at long times. This seems to indicate that the relaxation times fitted to the SAOSF data and steady shear data only do not capture the full range of characteristic time scales for the transient shear behavior. This is probably due to the limited range of the SAOSF experiment (0.01 to $100s^{-1}$), or else due to the fact that the SAOSF experiment does not probe N_1.

In Figure 7, we plot the elongational viscosity versus time for different elongation rates. The plot shows that the elongational viscosity increases with increas-

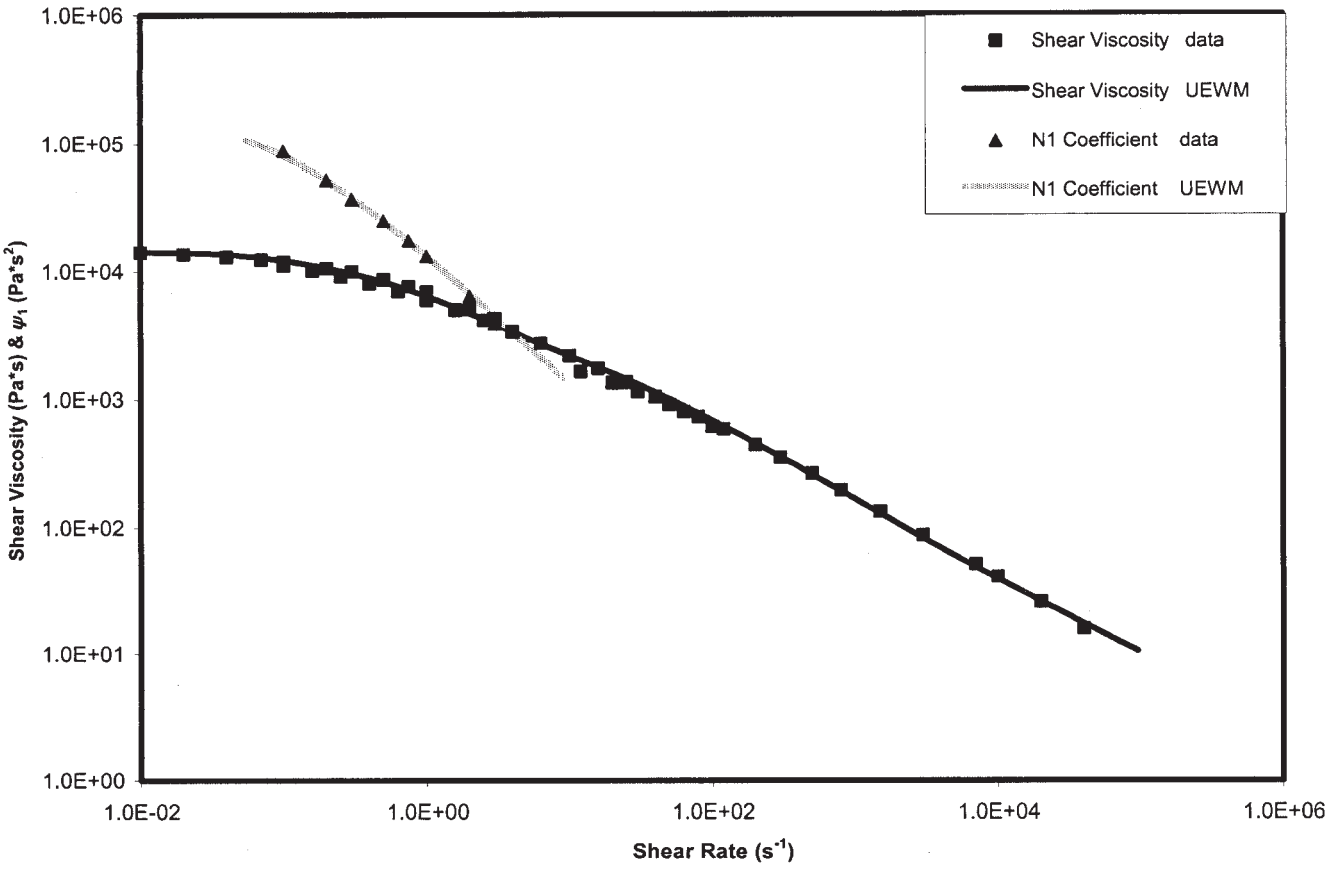

Figure 4 Steady-state shear viscosity and first normal stress coefficient versus shear rate, fitted with the UEWM Model.

TABLE VI
Ratio of the Second Normal Stress Coefficient to the First at Low Shear Rates for the Different Models

Model	UMM	UEWM	UGM	PCMM	PCMM-EWM	FCMM	FCMM-EWM
Ψ_2/Ψ_1	0	0	−9.82E−2	−9.15E−2	−4.52E−17	−9.20E−2	−1.34E−9

ing time and then reaches a steady-state value. Unfortunately, the theoretical predictions underestimate the experimental results, and actually fall below the Trouton curve (at a shear rate $0.01s^{-1}$); this is possible because the UEWM Model exhibits both thickening and thinning behavior of the elongational viscosity, depending on the choice of parameters.[4] The prediction obtained is actually better than the UMM Model prediction from an RMS perspective (see Table V), but still cannot be considered a success.

Uncoupled, nonlinear relaxation models

The next class of rheological models examined is that of uncoupled, nonlinear relaxation models. The example of this class studied here is the Uncoupled Giesekus Modes (UGM) Model. The constitutive equation for each mode stress tensor is taken as[5]:

$$\sigma^i_{\alpha\beta} + \lambda_i \hat{\sigma}^i_{\alpha\beta} + \frac{\alpha_i}{G^i_0}\,\sigma^i_{\alpha\gamma}\sigma^i_{\gamma\beta} = 2\eta_i A_{\alpha\beta}, \tag{8}$$

where $G^i_0 = n_i N_A k_B T$ and $\eta_i = n_i N_A k_B T \lambda_i$. The additional parameter, α, is the mobility factor, lying within the range $0 \leq \alpha \leq 1$. The total extra stress tensor is again given by the sum of the mode stress tensors, eq. (4). The dynamic moduli in SAOSF are still given by eqs. (5) and (6), since the nonlinear terms in the UGM Model do not contribute to the linear viscoelastic behavior.

Consistent fits for the data of dynamic moduli, shear viscosity, and first normal stress coefficient were obtained with this model; the parameter values thus obtained are reported in Table VII. Plots of these fits are quite similar to those of Figures 1 and 4. The RMS errors associated with these fits are reported in Table V.

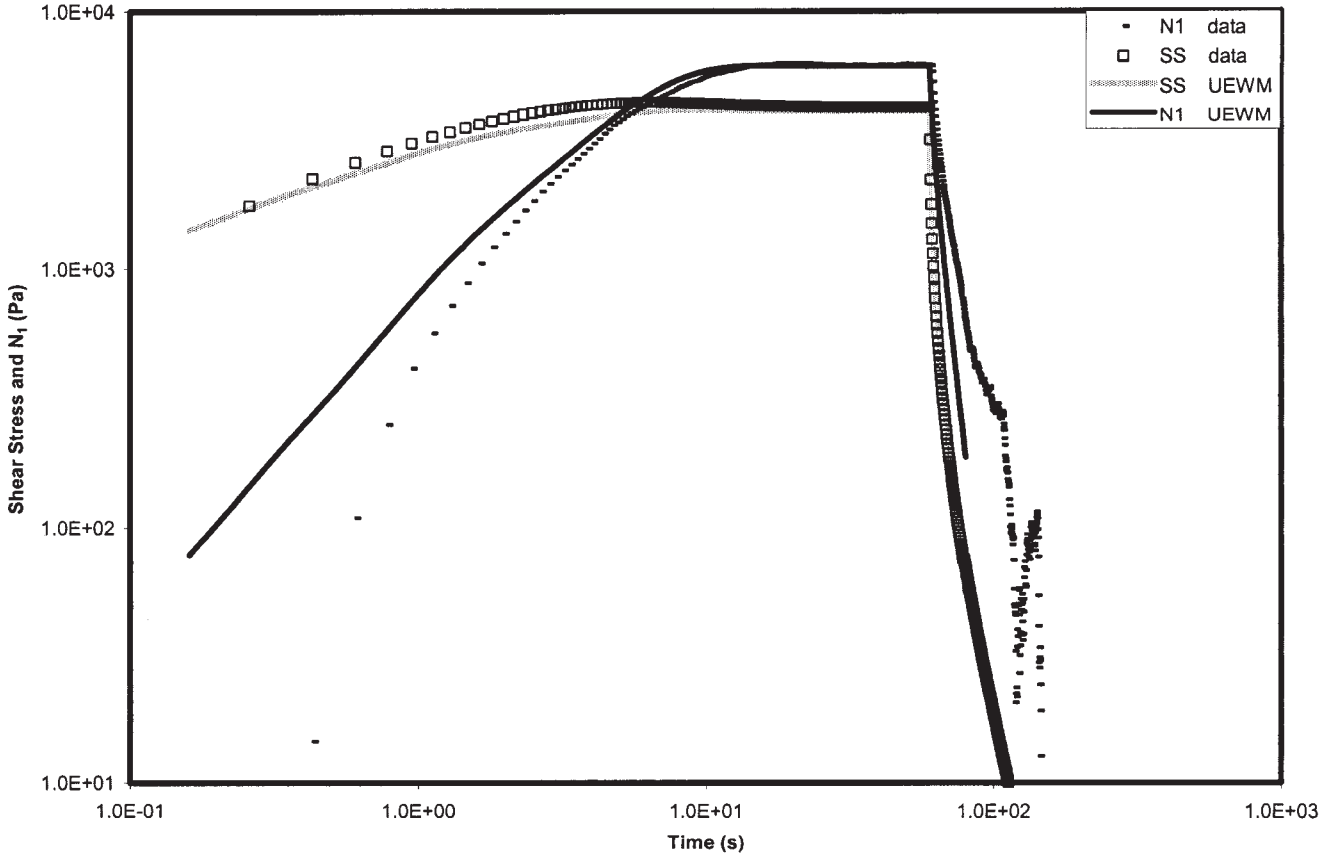

Figure 5 Transient stresses as a function of time, predicted with the UEWM Model for the LDPE melt ($\dot{\gamma} = 0.5\ s^{-1}$). SS refers to shear stress, and N1 refers to the first normal stress difference.

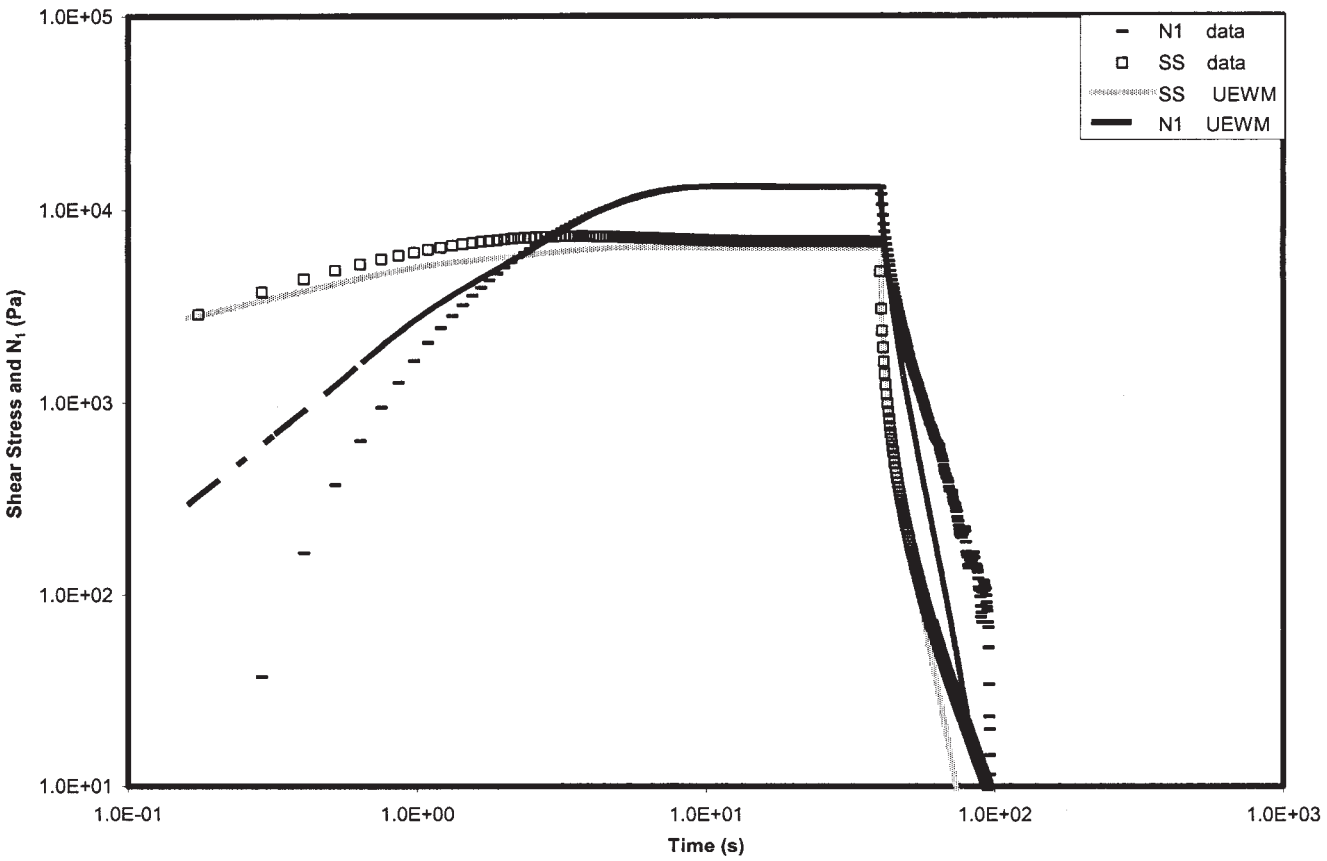

Figure 6 Transient stresses as a function of time, predicted with the UEWM Model ($\dot{\gamma} = 1.0\ s^{-1}$). SS refers to shear stress, and N1 refers to the first normal stress difference.

The zero shear rate value of $\Psi_2/\Psi_1 \approx -0.1$ predicted by the model is quite reasonable. (See Table VI for the exact value.) The transient shear stress under start-up and cessation of shear flow is also described well, as seen in Figures 8 and 9. The overshoot upon start-up of shear is quantitatively predicted in magnitude and duration. The relaxation behavior is quantitatively predicted at all but the longest times and highest shear rates for which data was obtained. At low values of shear rate (not presented in this article), the first normal stress difference predictions are also quite good. At higher values of the shear rate, as shown in Figures 8 and 9, the problems of the UEWM Model remain with regard to the very short and very long time behavior. Furthermore, the overshoot in N_1, barely apparent in the experimental data, is quite prominent in the model predictions. The magnitude of the predicted overshoot is roughly three times the magnitude of the experimental overshoot. As the shear rate is increased beyond $1s^{-1}$, this discrepancy tends to disappear as the experimental overshoot gains magnitude quickly. Unfortunately, measurements could not be obtained beyond $5s^{-1}$. One interesting point is that both the predictions and data attain a steady-state value at approximately the same point in time.

In Figure 10, we plot the elongational viscosity versus time for the different elongational rates. The predictions for this quantity are much better than those for the UEWM Model, but the steady-state values are still too low. This result is congruent with the generally accepted viewpoint that the Giesekus Model does a good job describing extensional flow characteristics.

Pair-wise coupled relaxation models

In this section, we begin to examine whether or not coupling between the various relaxation modes can contribute to the rheological response of a polymer melt. Intuitively, it seems evident that such would be the case; however, such a coupling is not going to be apparent in every rheological characterization experiment. For the present section, we limit our examination to models with pair-wise coupling between the various modes; that is, each mode can couple with one, and only one, additional mode. Our reasons for examining this case are discussed in the Introduction. However, we will look at two versions of pair-wise coupled relaxation models, the simplest possible version, the Pair-wise Coupled Maxwell Modes (PCMM) Model, and the Pair-Wise Coupled Maxwell Modes

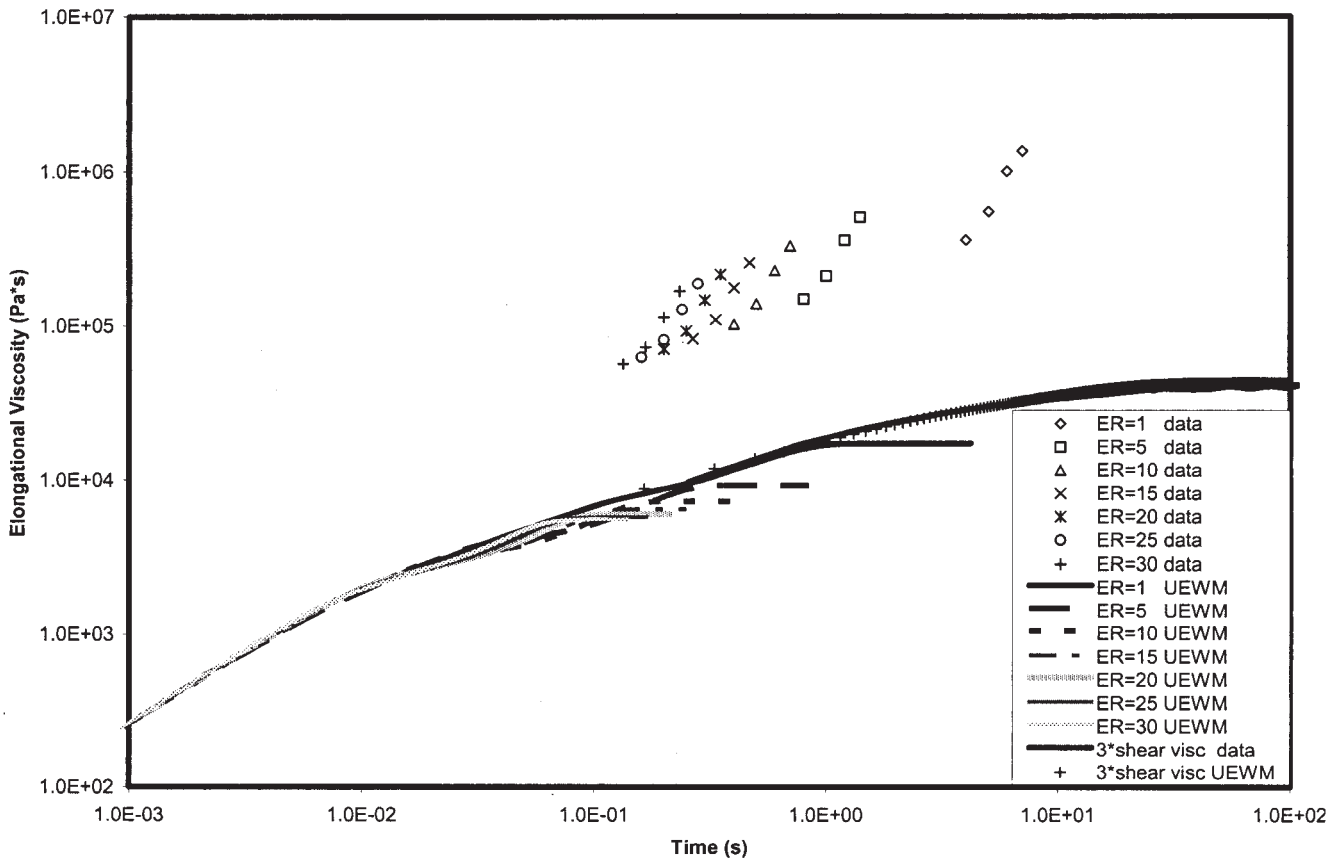

Figure 7 Elongational viscosity as a function of time, predicted with the UEWM Model. ER refers to the strain rate, in units of reciprocal seconds.

Model with the White/Metzner-like extension described above (PCMM-EWM).

The PCMM Model

The constitutive equations for the mode stress tensors in the PCMM Model are given by[11,25]:

$$\lambda_i \hat{\sigma}^i_{\alpha\beta} + \sigma^i_{\alpha\beta} + \theta_{ij} \frac{n_i}{n_j} \sqrt{\frac{n_i\lambda_i}{n_j\lambda_j}}\, \sigma^j_{\alpha\beta} + \frac{\theta_{ij}}{2n_j k_B T} \sqrt{\frac{n_i\lambda_i}{n_j\lambda_j}} (\sigma^i_{\alpha\gamma}\sigma^j_{\gamma\beta} + \sigma^j_{\alpha\gamma}\sigma^i_{\gamma\beta}) = 2\eta_i A_{\alpha\beta}, \quad (9)$$

where θ_{ij} is a coupling parameter that quantifies the degree of interaction between modes i and j. From experience,[1,26] the coupling parameters are required to lie within the interval, [0,1], but are typically small positive fractions. The evolution equation for mode j is the same as eq. (9) with the indices permuted. For a fluid modeled with 6 modes, there are three independent pairs of coupled evolution equations of this type. The total extra stress tensor is once again obtained through eq. (4).

The coupling in the PCMM Model affects the linear viscoelastic behavior[25]; hence, the complex modulus in SAOSF is no longer that of the UMM Model, but is given by

TABLE VII
List of Parameters for All Modes of the UGM Model Used To Fit the Data of Dynamic Moduli, Shear Viscosity, and First Normal Stress Coefficient

Mode no.	1	2	3	4	5	6
λ_i (s)	4.006E−4	9.481E−3	3.291E−2	8.672E−2	7.070E−1	7.795
n_i (mol/m^3)	7.714E+1	1.251E+1	1.354E−3	4.792	1.603	2.281E−1
α_i	1.862E−1	8.930E−1	3.375E−20	3.926E−1	9.193E−1	1.540E−1

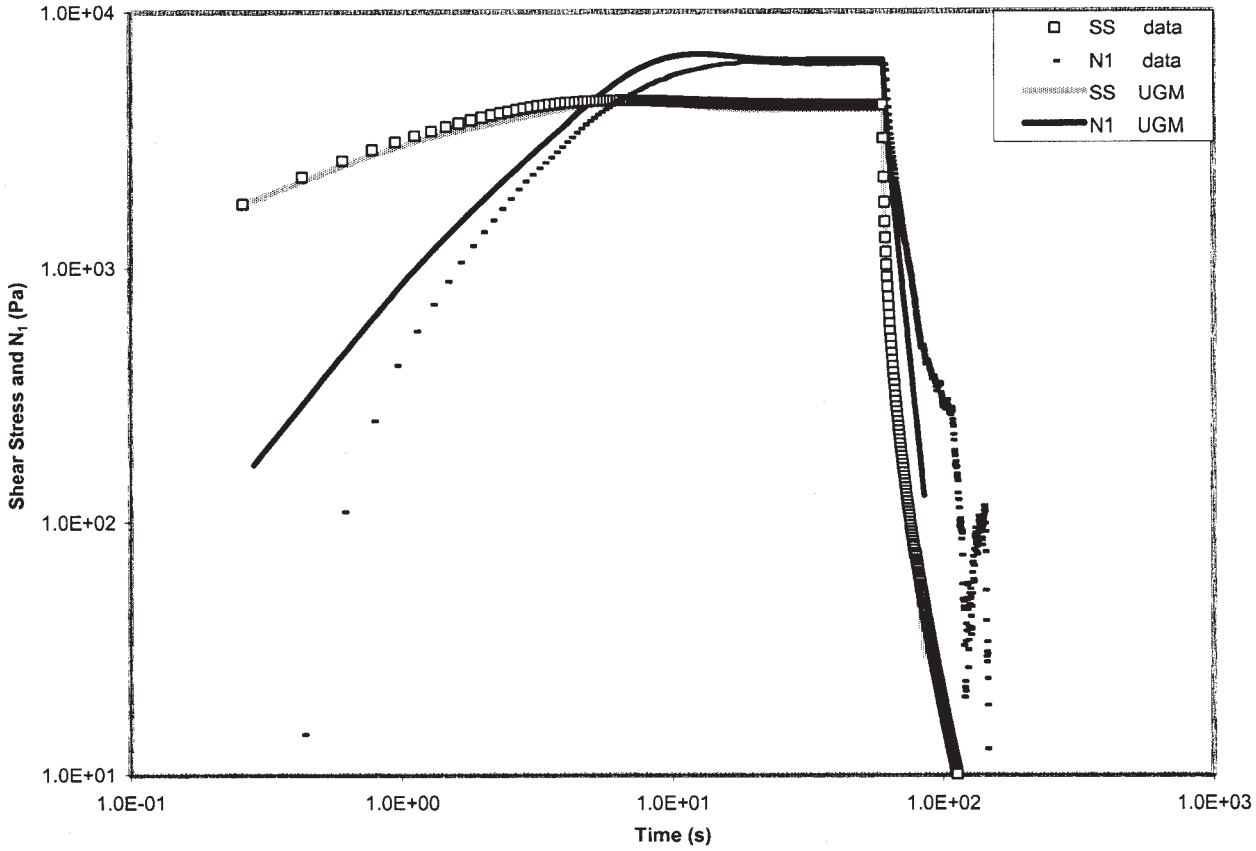

Figure 8 Transient stresses as a function of time, as predicted with the UGM Model ($\dot{\gamma} = 0.5\ s^{-1}$).

$$\frac{G_{ij}}{i\omega} = \frac{\eta_i(De_j i + 1) + \eta_j(De_i i + 1) - \sqrt{\eta_i\eta_j}\theta_{ij}\chi_{ij}}{(1 - De_i De_j) + i(De_i + De_j) - \theta_{ij}^2}, \quad (10)$$

where

$$De_i \equiv \omega\lambda_i, \text{ and } \chi_{ij} = \frac{\eta_i De_j}{\eta_j De_i} + \frac{\eta_j De_i}{\eta_i De_j}. \quad (11)$$

Note that eq. (10) applies to each pair of modes, so that the total complex modulus is given by the sum of three quantities. In the limit of $\theta_{ij} \to 0$, it can be shown that eq. (10) reduces to the complex modulus of the UMM Model, eqs. (5) and (6).

The PCMM Model was studied extensively by Jiang et al.,[1] and was found to be a very peculiar model. It was used as the test case for our preliminary study, and so will only be discussed very briefly here. The fits to the dynamics moduli, steady shear viscosity, and first normal stress coefficient display a characteristic waviness.[1] The cause of this is the inherently linear nature of the Maxwell relaxation modes; that is, without the coupling parameter, the model reduces to the UMM Model, with all of its associated problems arising from its linear responses. In order for the PCMM Model to fit the shear-thinning behavior of η or N_1, it is necessary for this model to have nonzero values of the coupling parameters, θ_{ij}. Consequently, the model must set the concentration of 1 mode of each pair (the one with the shorter relaxation time) to zero to produce artificially the shear-thinning behavior. Thus, one really obtains only a 3-mode fit (since only 3 modes influence the stress tensor) of the complex modulus, thus producing the inherent waviness. For more details as to this phenomenon, please refer to the previous article.[1]

Because of the waviness of the steady shear data, the RMS error of these curves is much greater than the previous cases. Consequently, predictions of the transient shear and elongational behavior are also subject to errors, and nothing is to be gained by presenting them. It is interesting, however, that the prediction for the ratio of normal stress coefficients is approximately −0.09.

The PCMM-EWM Model

One might expect that replacing the constant relaxation times in the PCMM Model with the White/Metzner extension of eq. (7) could alleviate the problems reported in the preceding subsection. This would relieve the smaller relaxation time modes of each pair of the necessity of having a null value for their con-

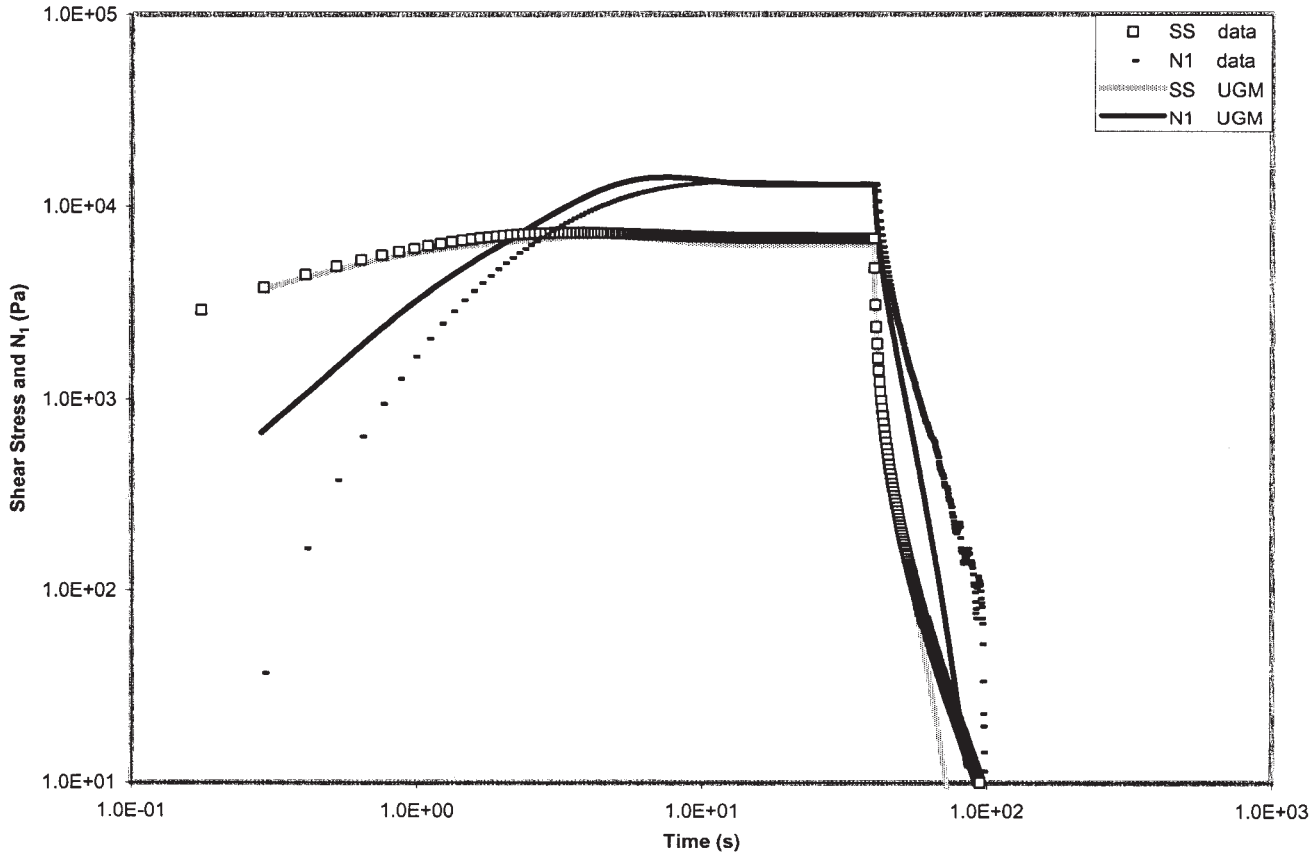

Figure 9 Transient stresses as a function of time, as predicted with the UGM Model ($\dot{\gamma} = 1.0\ s^{-1}$).

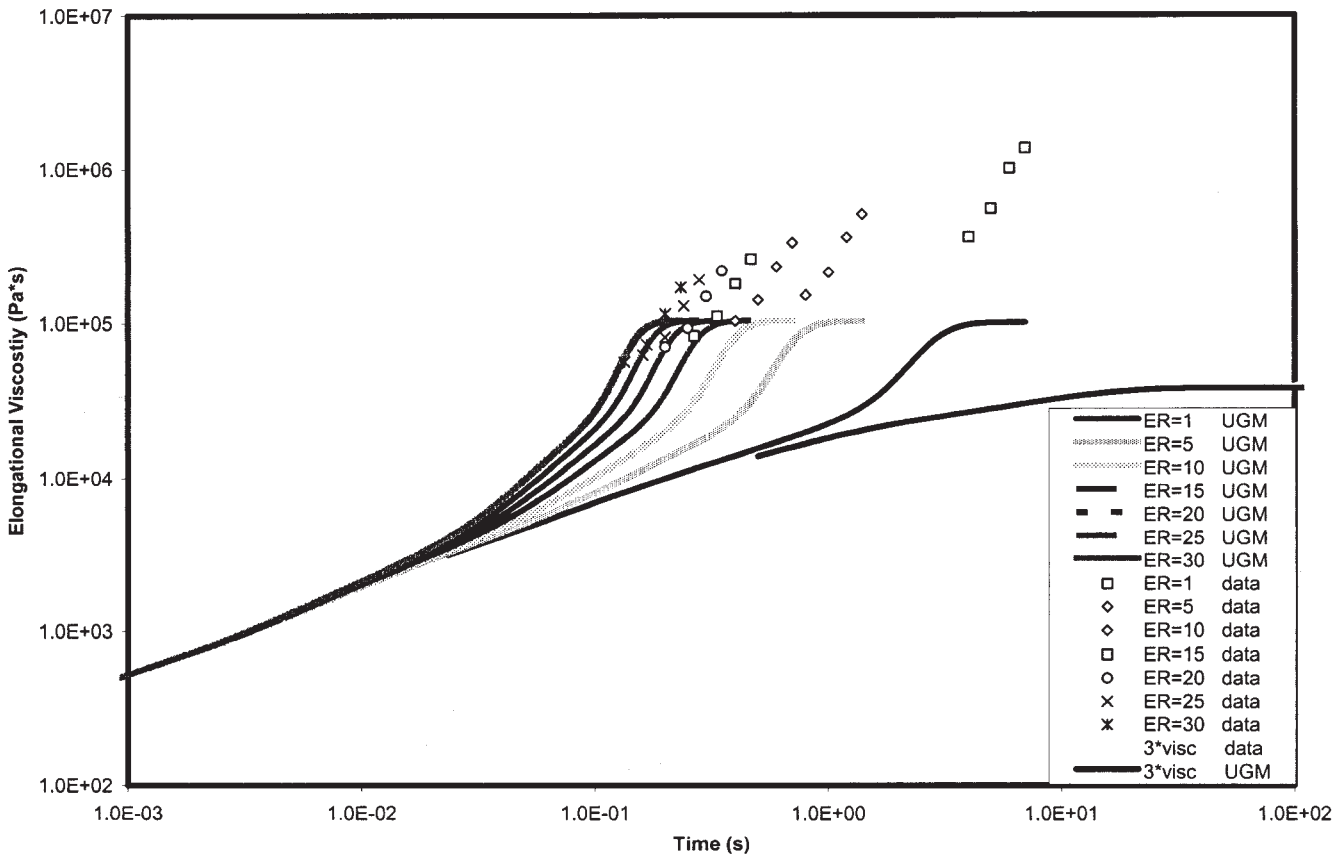

Figure 10 Elongational viscosity as a function of time, as predicted with the UGM Model.

TABLE VIII
List of Parameters for All Modes of the PCMM-EWM Model Used To Fit the Data of Complex Modulus, Shear Viscosity, and First Normal Stress Coefficient

Mode no.	1	2	3	4	5	6
$\lambda_{0,i}$ (s)	1.013E−5	4.313E−1	5.314E−4	3.284E−2	3.569E−3	6.933
n_i (mol/m^3)	1.313E−6	2.538	4.728E−11	8.428	2.180E+1	3.331E−1
k_i	−1.073E−14	−3.605	−1.797E+1	−4.690E−4	−1.866	−5.236E−1
θ_{ij}	3.909E−18		3.000E−18		4.196E−18	

centration parameters, since the EWM nonlinearity would produce the requisite shear-thinning behavior. This expectation was tested, with the following results.

The constitutive equations for the mode stress tensors in this case are the same as eq. (9) above, with eq. (7) inserted for the mode relaxation times. The equation for the complex modulus, eq. (10), is not affected by this insertion, since it is a linearized expression. Using these equations, the model was fitted to the same data as prior cases, and the parameters reported in Table VIII were obtained. Note that the modal concentrations of the shorter relaxation times are not necessarily null-valued now. The fits obtained with these parameter values for the dynamic moduli, shear viscosity, and first normal stress coefficient are very similar to those of Figures 1 and 4, and are not presented. The RMS errors of the fits are reported in Table V.

Predictions for the transient shear and elongational behavior are presented in Figures 11 to 13. The shear behavior is similar to that of the UGM Model, whereas the elongational prediction has improved over that of the UGM Model. Interestingly, the value of the normal stress ratio has dropped to zero (see Table VI). Note that the coupling parameter values in Table VIII are all very small, indicating that this model performs similarly to the UEWM Model. The only effect of the coupling thus appears to be on the elongational viscosity. These trends will be considered in greater detail in the discussion below.

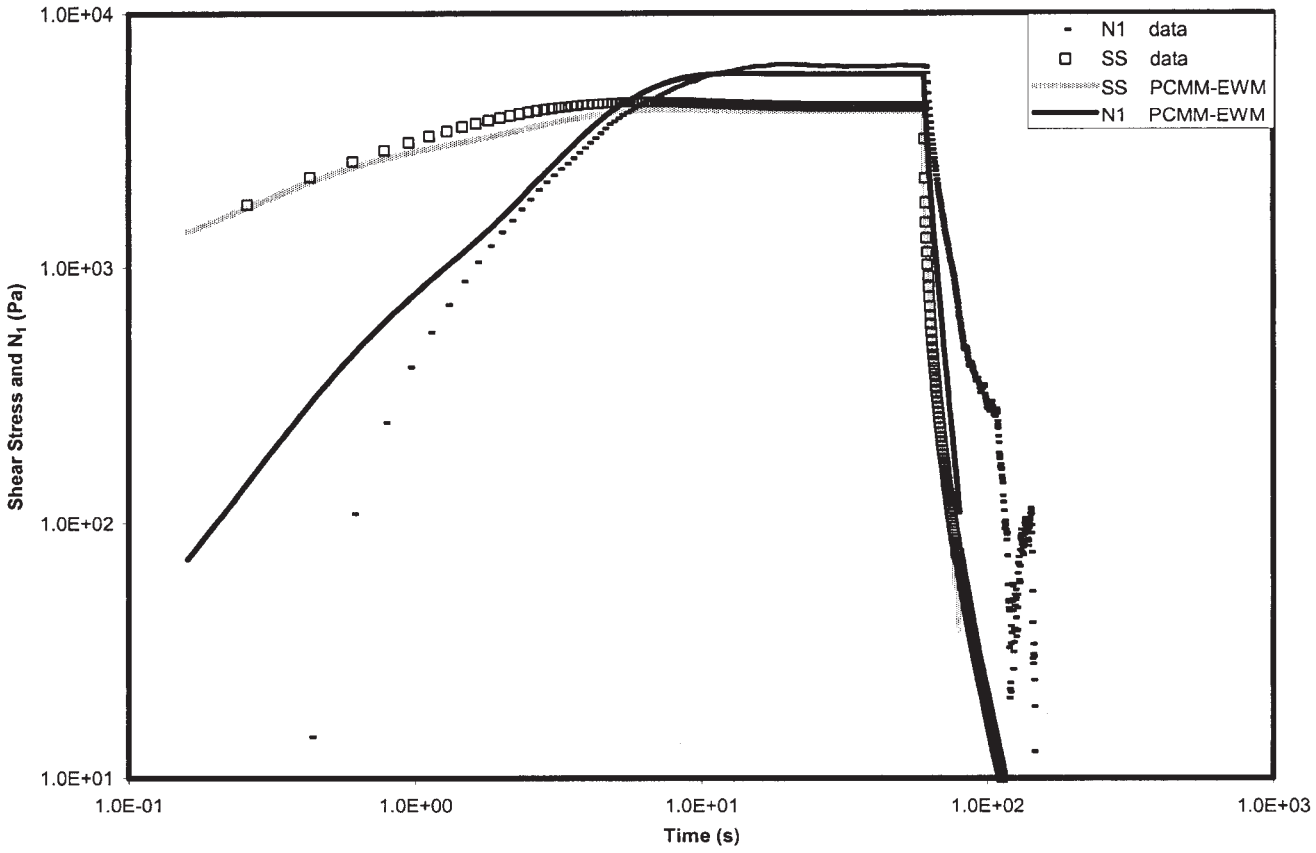

Figure 11 Transient shear stress as a function of time, as predicted with the PCMM-EWM Model ($\dot{\gamma} = 0.5\ s^{-1}$).

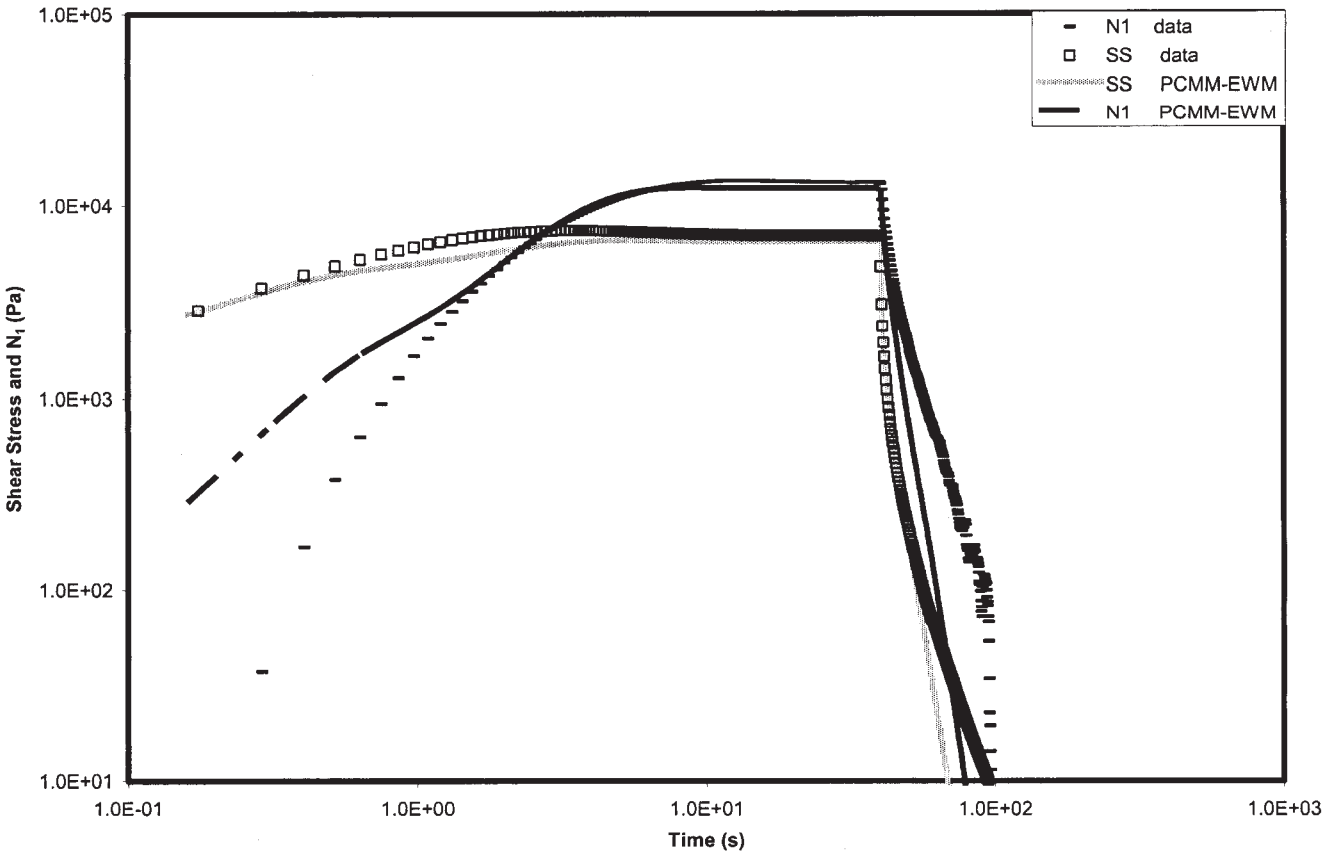

Figure 12 Transient shear stress as a function of time, as predicted with the PCMM-EWM Model ($\dot{\gamma} = 1.0\ s^{-1}$).

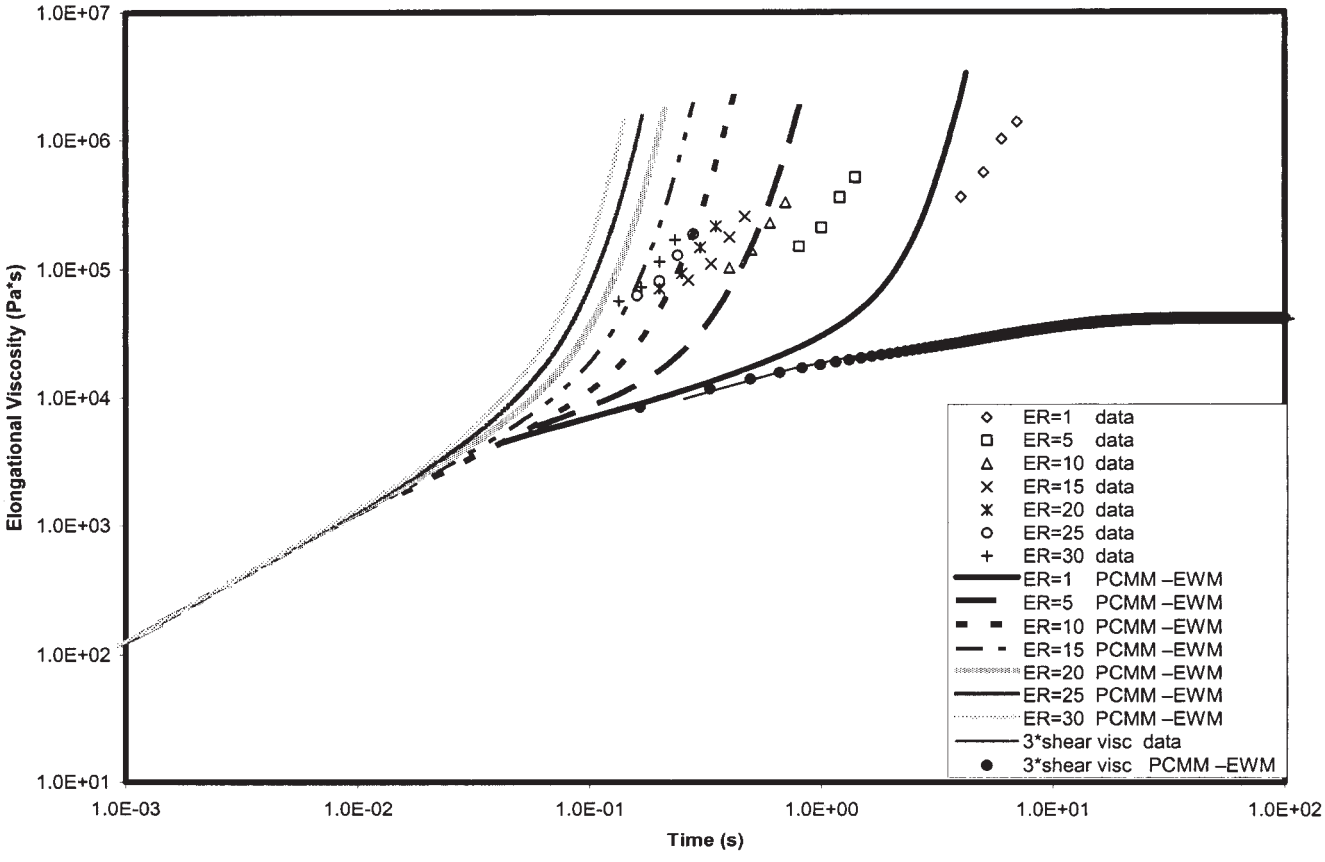

Figure 13 Elongational viscosity as a function of time, as predicted with the PCMM-EWM Model.

Fully-Coupled relaxation models

The obvious generalization of the PCMM Models is to allow full coupling between all of the mode stress tensors. Thus, we examine a Fully-Coupled Maxwell Modes (FCMM) Model, as well as an FCMM Model with the White/Metzner-like extension (FCMM-EWM Model). It is highly likely that such generality will not be necessary, and that only some modes will interact with each other. Here, we allow the optimization methodology to choose the degree of coupling necessary to fit the requisite experimental data. As seen below, many of the coupling parameters turn out to be negligibly small, indicating effectively no interactions between the corresponding relaxation modes.

The FCMM Model

In this model, the constitutive equations for the mode stress tensors are given by[11]

$$\lambda_i \hat{\sigma}^j_{\alpha\beta} + \sigma^i_{\alpha\beta} + \sum_{j=1,j\neq i}^{6} \theta_{ij} \frac{n_i}{n_j} \sqrt{\frac{n_i\lambda_i}{n_j\lambda_j}}\, \sigma^j_{\alpha\beta} + \sum_{j=1,j\neq i}^{6} \frac{\theta_{ij}}{2n_j k_B T} \sqrt{\frac{n_i\lambda_i}{n_j\lambda_j}} \left(\sigma^i_{\alpha\gamma}\sigma^j_{\gamma\beta} + \sigma^j_{\alpha\gamma}\sigma^i_{\gamma\beta}\right) = 2\eta_i A_{\alpha\beta}. \tag{12}$$

For a given number of modes, n, the dynamical moduli in SAOSF can be calculated according to the linear equation

$$[G'_1, \ldots, G'_n, G''_1, \ldots, G''_n]^T = \mathbf{M}^{-1} \cdot [0, \ldots, 0, \eta_1\omega, \ldots, \eta_n\omega]^T, \tag{13}$$

where

$$\mathbf{M} = \begin{bmatrix} 1 & \theta_{12}\frac{n_1}{n_2}\sqrt{\frac{n_1\lambda_1}{n_2\lambda_2}} & \cdots & \theta_{1n}\frac{n_1}{n_n}\sqrt{\frac{n_1\lambda_1}{n_n\lambda_n}} & -\lambda_1\omega & 0 & \cdots & 0 \\ \theta_{21}\frac{n_2}{n_1}\sqrt{\frac{n_2\lambda_2}{n_1\lambda_1}} & 1 & \cdots & \theta_{2n}\frac{n_2}{n_n}\sqrt{\frac{n_2\lambda_2}{n_n\lambda_n}} & 0 & -\lambda_2\omega & \cdots & 0 \\ \vdots & \vdots & \vdots & \vdots & \vdots & \vdots & \vdots & \vdots \\ \theta_{n1}\frac{n_n}{n_1}\sqrt{\frac{n_n\lambda_n}{n_1\lambda_1}} & \theta_{n2}\frac{n_n}{n_2}\sqrt{\frac{n_n\lambda_n}{n_2\lambda_2}} & \cdots & 1 & 0 & 0 & \cdots & -\lambda_n\omega \\ -\lambda_1\omega & 0 & \cdots & 0 & 1 & \theta_{12}\frac{n_1}{n_2}\sqrt{\frac{n_1\lambda_1}{n_2\lambda_2}} & \cdots & \theta_{1n}\frac{n_1}{n_n}\sqrt{\frac{n_1\lambda_1}{n_n\lambda_n}} \\ 0 & -\lambda_2\omega & \cdots & 0 & \theta_{21}\frac{n_2}{n_1}\sqrt{\frac{n_2\lambda_2}{n_1\lambda_1}} & 1 & \cdots & \theta_{2n}\frac{n_2}{n_n}\sqrt{\frac{n_2\lambda_2}{n_n\lambda_n}} \\ \vdots & \vdots & \vdots & \vdots & \vdots & \vdots & \vdots & \vdots \\ 0 & 0 & \cdots & -\lambda_n\omega & \theta_{n1}\frac{n_n}{n_1}\sqrt{\frac{n_n\lambda_n}{n_1\lambda_1}} & \theta_{n2}\frac{n_n}{n_2}\sqrt{\frac{n_n\lambda_n}{n_2\lambda_2}} & \cdots & 1 \end{bmatrix}. \tag{14}$$

The FCMM Model has the same problem as the PCMM Model, namely, the linear Maxwell-type relaxation is not adequate to capture the shear-thinning behavior of the steady shear flow properties. Consequently, a fit of the moduli, shear viscosity, and first normal stress coefficient again reveals that all but one (at most) of the coupling parameters are negligibly small. This is required to reproduce artificially the necessary shear-thinning characteristics. As a consequence, the fits again display the wavy nature of the PCMM Model fits.[1] All other characteristics are similar to the PCMM Model, described above.

The FCMM-EWM Model

The last model examined here is the FCMM-EWM Model, wherein the relaxation times in eqs. (12) to (14) are replaced with the EWM relaxation time of eq. (7). Parameter fits to the moduli, viscosity, and first normal stress coefficient are again very similar to those presented in Figures 1 and 4, and RMS errors are reported in Table V. Tables IX and X contain the optimized parameter values. Note from Table X that many of the coupling parameters are still chosen to be zero, although there is a definite trend away from pair-wise coupling.

Predictions for the transient shear and elongational stresses are presented in Figures 14 to 16. RMS errors are collected in Table V. The predictions are quite good for the shear properties, except again for N_1 at very short and very long times. The elongational viscosity predictions display the correct qualitative trends, but are not particularly good. The ratio of the normal stress coefficients is very small.

TABLE IX
List of Non-Coupling Parameters for All Modes of the FCMM-EWM Model Used To Fit the Data of Complex Modulus, Shear Viscosity, and First Normal Stress Coefficient

Mode no.	1	2	3	4	5	6
$\lambda_{0,i}$ (s)	1.637E−4	2.391E−2	3.153E−2	1.015E+1	1.585	2.346E−1
n_i (mol/m^3)	7.076E−4	3.461E+1	7.329	1.347E−1	7.747E−1	2.693
k_i	−9.009E−2	−2.670	−1.320E2	−4.564E−1	−9.662E−1	−4.049

Comparison of model performances

RMS errors for the various models in the different experiments are summarized in Table V. Overall, it is evident that the UGM and FCMM-EWM Models provide the best fitting and predictive capabilities of the models tested. Although the UGM Model has a lower RMS error for elongational viscosity than the FCMM-EWM Model, this is probably due simply to the fact that the former model under-predicts the viscosity, whereas the latter model over-predicts it. Qualitatively, the FCMM-EWM Model provides more esthetically appealing fits of this quantity.

Thus, overall, the UGM and FCMM-EWM Models are the best models examined herein, although the FCMM-EWM Model contains the highest number of parameters (see Table I): the UGM Model has 18 parameters, and the FCMM-EWM Model has 48 parameters. Note, however, that the optimized fit of the FCMM-EWM Model has only 28 non-negligible parameters, whereas the UGM Model has 17 non-negligible parameters. Hence, the FCMM-EWM Model is being fit with only about half of its inherent parameters. This model is also the most complex, and one must wonder at present whether or not this additional complexity is necessary. Unfortunately, the experiments performed herein are probably not the best ones to help answer this question. Double-strain experiments (currently underway), wherein one might expect to see dramatic mode coupling effects, will provide a more complete picture of this aspect of the modeling.

Another interesting observation regarding the model behavior presented above is that the UGM Model gives a reasonable value of Ψ_2/Ψ_1, as do the PCMM and FCMM Models. It is noteworthy that the FCMM-EWM Model does not. The source of this inadequacy is most likely due to the use of the White/Metzner (WM) extension; remember that the UEWM Model still retained a null ratio. It thus seems plausible that having a reasonable value of this ratio is controlled by the nonlinear (quadratic) relaxation terms in the UGM Model. In the coupled models without the WM extension, a reasonable value is obtained because the nonlinear relaxation effect is not washed out by the WM modifications. This gives some minor indication that perhaps coupling effects (which are highly nonlinear) can affect steady shear elastic properties such as Ψ_2, assuming that the uncoupled nonlinear models are merely mimicking the effects of the coupled models. More investigation will hopefully yield a definitive answer to this puzzle.

CONCLUSIONS

The potential of rheological models to fit and predict experimental data was investigated in this article. For a series of models, parameter fits were generated by a numerical optimization procedure by fitting to experimental data from SAOSF and steady shear flow. Model predictions were then obtained for transient shear and elongational flows, and these were compared with available experimental data. Some models perform very well in one or two types of flows, although none of models can perform perfectly in all types of flows. All of the models examined herein were very simple, semiphenomenological models, and were only used as representatives of the various classes of rheological models in use today. Nevertheless, the outlook seems bright for addressing the inadequacies of rheological constitutive equations and

TABLE X
List of Coupling Parameters for All Modes of the FCMM-EWM Model Used To Fit the Data of Complex Modulus, Shear Viscosity, and First Normal Stress Coefficient

θ_{ij}	1	2	3	4	5	6
1	—	2.215E−12	1.284E−20	1.781E−20	1.122E−10	1.787E−10
2	2.215E−12	—	1.082E−19	1.212E−20	1.316E−20	2.408E−20
3	1.284E−20	1.082E−19	—	1.236E−20	1.185E−20	4.121E−12
4	1.781E−20	1.212E−20	1.236E−20	—	1.854E−20	8.720E−9
5	1.122E−10	1.316E−20	1.185E−20	1.854E−20	—	6.446E−20
6	1.787E−10	2.408E−20	4.121E−12	8.720E−9	6.446E−20	—

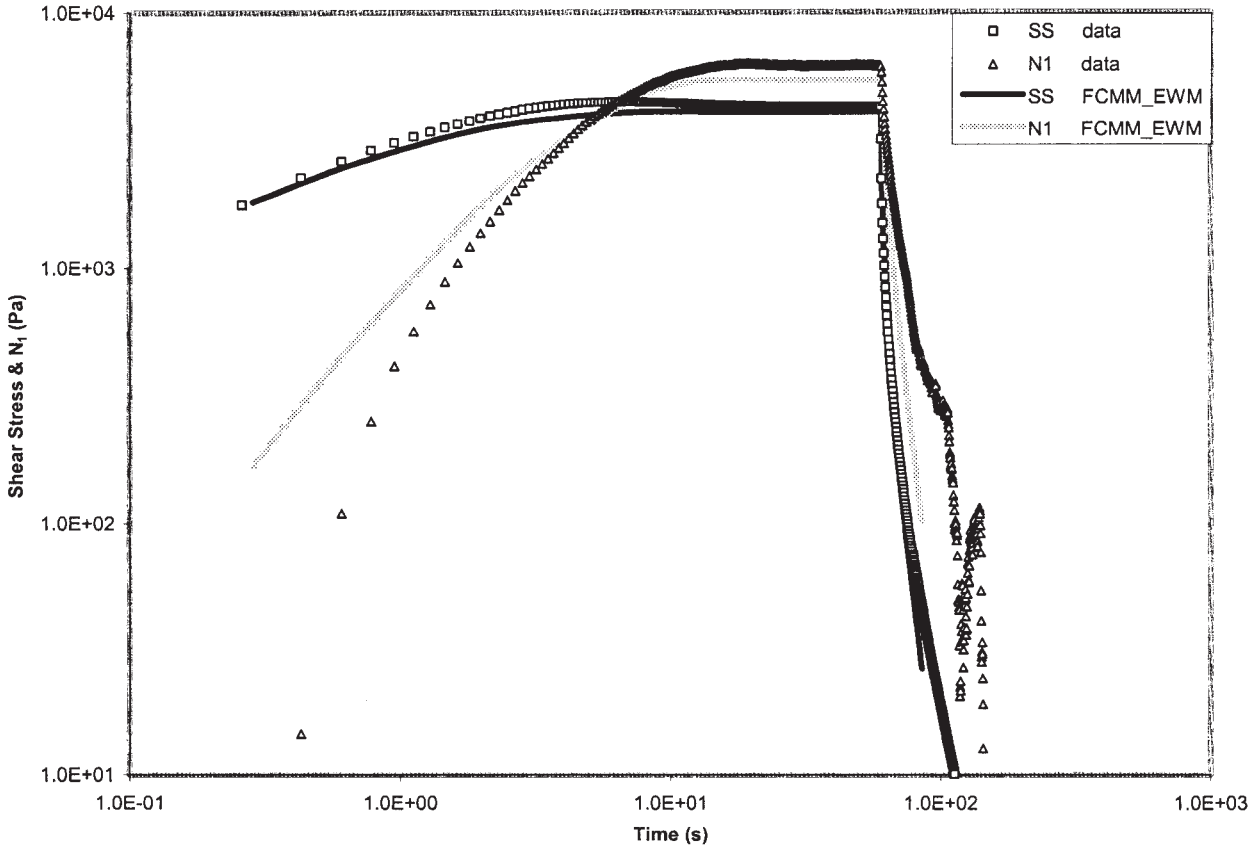

Figure 14 Transient stresses as functions of time, as predicted with the FCMM-EWM Model ($\dot{\gamma} = 0.5\ s^{-1}$).

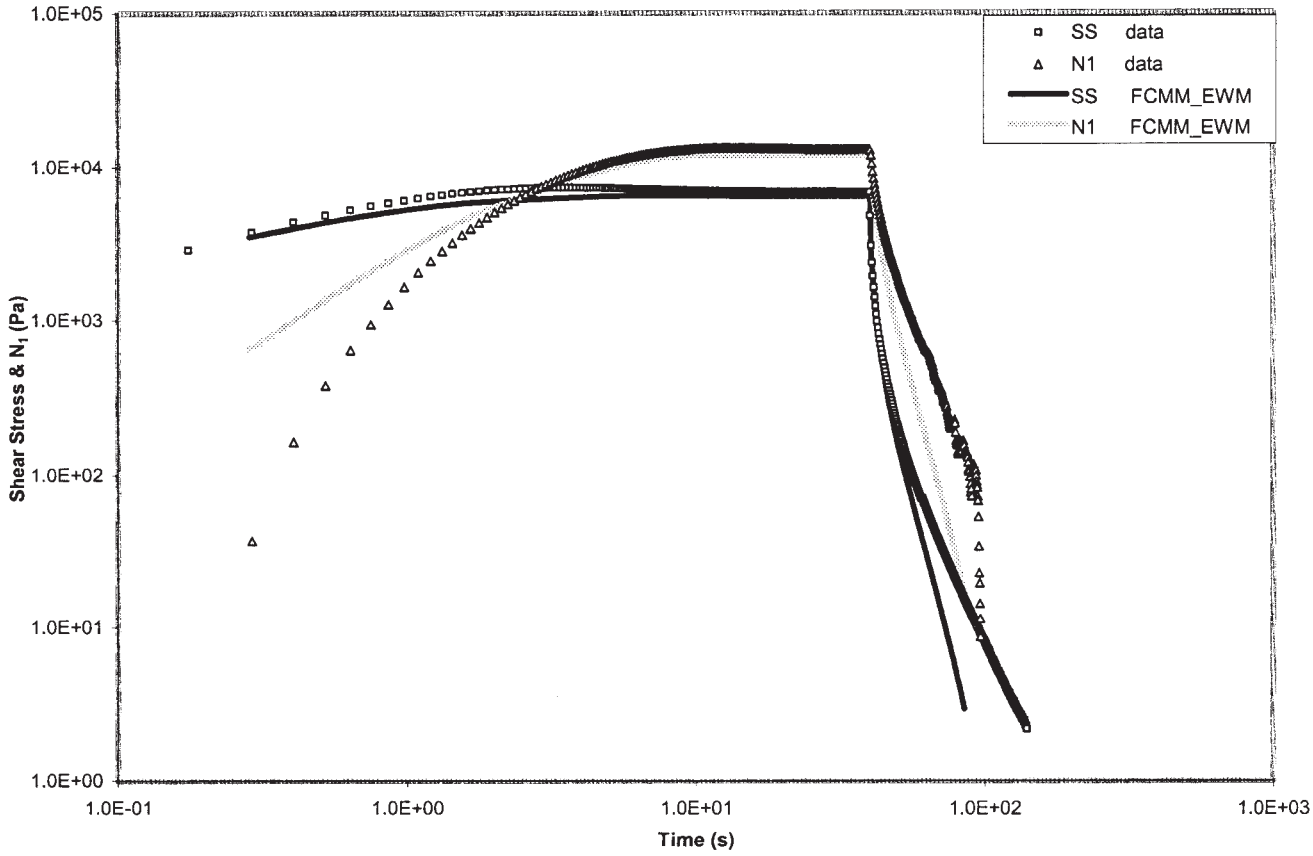

Figure 15 Transient stresses as functions of time, as predicted with the FCMM-EWM Model ($\dot{\gamma} = 1.0\ s^{-1}$).

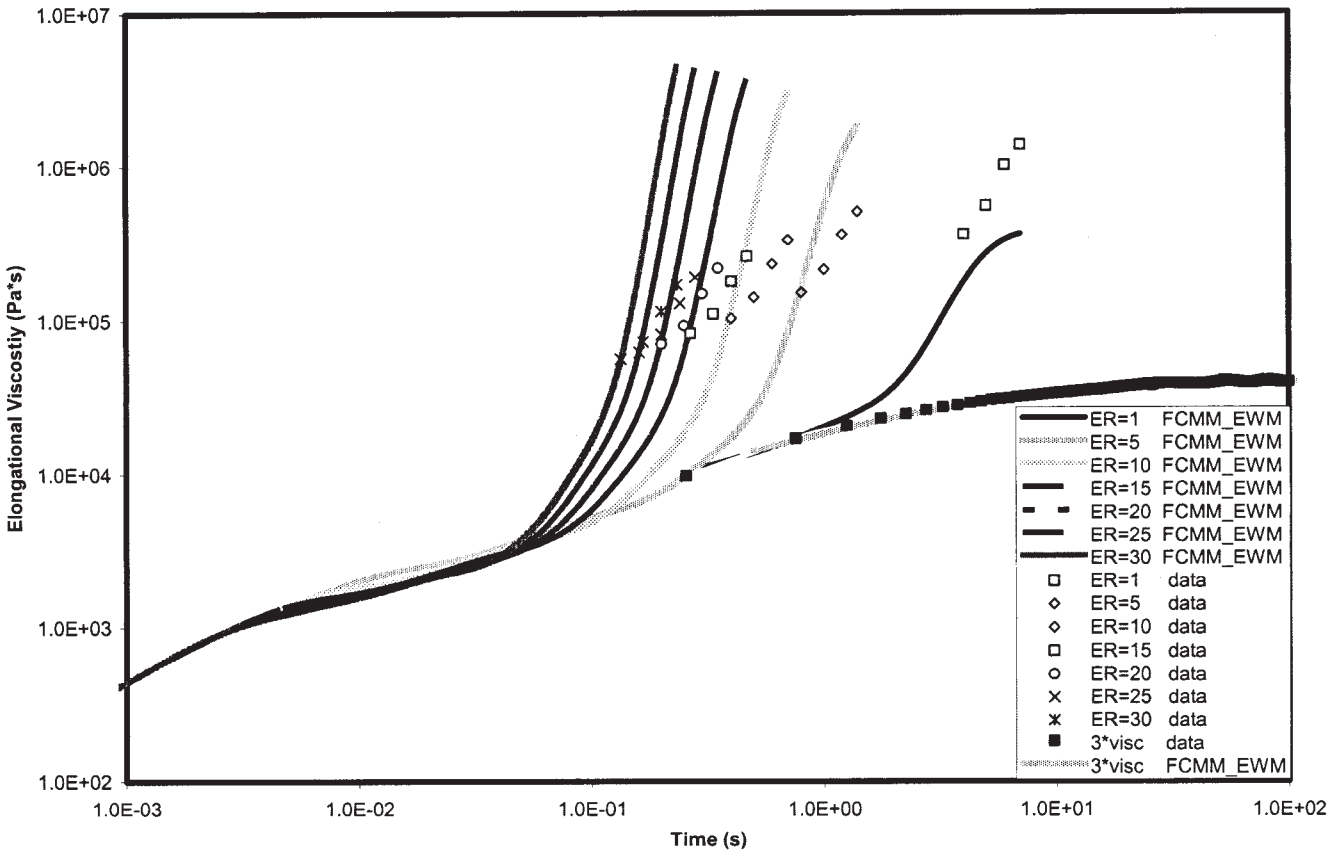

Figure 16 Elongational viscosity as a function of time, predicted with the FCMM-EWM Model.

potentially describing real materials with unprecedented accuracy. Such an event would be well worth pursuing.

We thank Drs. Simhambhatla and Leonov for allowing us to use their Padé-Laplace program *PADLAP* for determining the base-case linear viscoelastic parameters.

References

1. Jiang, B.; Kamerkar, P. A.; Keffer, D. J.; Edwards, B. J. J Non-Newtonian Fluid Mech 2004, 120, 11.
2. Phan-Thien, N.; Tanner, R. I. J Non-Newtonian Fluid Mech 1977, 2, 353.
3. Apelian, M. R.; Armstrong, R. C.; Brown, R. A. J Non-Newtonian Fluid Mech 1988, 27, 299.
4. Souvaliotis, A.; Beris, A. N. J Rheol 1992, 36, 241.
5. Giesekus, H. J Non-Newtonian Fluid Mech 1982, 11, 69.
6. McLeish, T. C. B.; Larson, R. G. J Rheol 1998, 42, 81.
7. Inkson, N. J.; McLeish, T. C. B.; Harlen, O. G.; Groves, D. J. J Rheol 1999, 43, 873.
8. Lee, K.; Mackley, M. R.; McLeish, T. C. B.; Nicholson, T. M.; Harlen, O. G. J Rheol 2001, 45, 1261.
9. Chodankar, C. D.; Schieber, J. D.; Venerus, D. C. Rheol Acta 2003, 42, 123.
10. Chodankar, C. D.; Schieber, J. D.; Venerus, D. C. J Rheol 2003, 47, 413.
11. Beris, A. N.; Edwards, B. J. Thermodynamics of Flowing Systems; Oxford University Press: New York, 1994.
12. Quinzani, L. M.; McKinley, G. H.; Brown, R. A.; Armstrong, R. C. J Rheol 1990, 34, 705.
13. Agassant, J. F.; Baaijens, F.; Bastian, H.; Bernnat, A.; Bogaerds, A. C. B.; Coupez, T.; Debbaut, B.; Gavrus, A. L.; Goublomme, A.; van Gurp, M.; Koopmans, R. J.; Laun, H. M.; Lee, K.; Nouatin, O. H.; Mackley, M. R.; Peters, G. W. M.; Rekers, G.; Verbeeten, W. M. H.; Vergnes, B.; Wagner, M. H.; Wassner, E.; Zoetelief, W. F. Intern Polym Process 2002, 17, 3.
14. Langouche, L.; Debbaut, B. Rheol Acta 1999, 38, 48.
15. Debbaut, B.; Dooley, J. J Rheol 1999, 43, 1525.
16. Feigl, K.; Tanner, F. X.; Edwards, B. J.; Collier, J. R. J Non-Newtonian Fluid Mech 2003, 115, 191.
17. Collier, J. R.; Wei, X.; Petrovan, S.; Hudson, N. In preparation.
18. Simhambhatla, M.; Leonov, A. I. Rheol Acta 1993, 32, 589.
19. Press, W. H.; Tevkolsky, S. A.; Flannery, B. P. Numerical Recipes in Fortran 77; Cambridge University Press: Cambridge, 1992.
20. Honerkamp, J. Rheol Acta 1989, 28, 363.
21. Orbey, N.; Dealy, J. M. J Rheol 1991, 35, 1035.
22. Fulchiron, R.; Verney, V.; Cassagnau, P.; Michel, A.; Levoir, P.; Aubard, J. J Rheol 1993, 37, 17.
23. Thimm, W.; Friedrich, C.; Marth, M.; Honerkamp, J. J Rheol 1999, 43, 1663.
24. He, L.; Ding, R.; Leonov, A. I.; Dixon, H.; Quirk, R. P. J Appl Polym Sci 1999, 71, 1315.
25. Edwards, B. J.; Beris, A. N.; Mavrantzas, V. G. J Rheol 1996, 40, 917.
26. Edwards, B. J.; Keffer, D. J.; Reneau, C. W. J Appl Polym Sci 2002, 85, 1714.